

Weak Neutral Current Axial Form Factor and (Anti)Neutrino-Nucleon Scattering

Raza Sabbir Sufian¹, Keh-Fei Liu², David G. Richards¹

¹*Theory Center, Jefferson Lab, 12000 Jefferson Avenue, Newport News, VA 23606, USA*

²*Department of Physics and Astronomy, University of Kentucky, Lexington, Kentucky 40506, USA*

The interplay of first-principles lattice QCD calculations and experimental results can unveil such nucleon properties to higher precision and accuracy than either theory or experiment alone can obtain. In this simple yet novel analysis, using a combination of the strange quark electromagnetic form factors from lattice QCD and (anti)neutrino-nucleon neutral current elastic scattering differential cross section data from MiniBooNE experiments in a kinematic region $0.3 \lesssim Q^2 \lesssim 0.7$ GeV², we obtain, (1) the most precise determination of the weak neutral current axial form factor with weak axial charge $G_A^Z(0) = -0.734(63)(20)$, (2) strange quark contribution to the proton spin $\Delta s = -0.196(127)(41)$, (3) reconstruct the MiniBooNE data along with the prediction of BNL E734 (anti)neutrino-nucleon scattering differential cross section data in the $0 \lesssim Q^2 \leq 1$ GeV² momentum transfer region to test the validity and predictive power of this calculation. This analysis can play an important role in disentangling the nuclear effects in the neutrino-nucleus scattering processes.

Precision measurements of various matrix elements associated with (anti)neutrino-nucleon $(\bar{\nu})\nu - N$ scattering can directly impact a wide variety of physical processes. These include, but are not limited to, understanding of solar neutrino [1–3] and atmospheric [4–6] neutrino oscillations, three non-vanishing mixing angles [7, 8] resulting in a phase violating CP asymmetry leading to the matter-antimatter asymmetry in the universe in the three-neutrino framework, dynamics of neutron-rich core-collapse supernovae [9, 10], the axial-sector structure of and strange quark (s -quark) contribution Δs to the proton spin, and non-standard interactions leading to beyond-the-standard-model physics [11]. One such matrix element is the weak neutral current (WNC) axial form factor (FF) G_A^Z , arising through the exchange of neutral Z^0 -boson between the lepton and quarks.

The value of G_A^Z is not constrained from parity-violating electron-proton scattering experiments at backward angles [12–16] due to the lack of knowledge of its Q^2 -behavior and the suppression of the tree-level electroweak radiative correction (RC). Furthermore, RCs involving strong interaction can be larger than $\mathcal{O}(\alpha_s)$ [17] are not known theoretically. For example, using theoretical constraints from Ref. [17] and dipole form [18] for the isovector $G_A^{Z,T=1}$ and isoscalar $G_A^{Z,T=0}$ FFs, the value of proton $G_A^Z = -0.59(34)$ was used in the analysis of the most recent measurement of the weak charge of the proton by the Q_{weak} Collaboration [19].

Unlike charged current quasi-elastic (CCQE) scattering which is sensitive only to the isovector current, neutral current elastic (NCE) $(\bar{\nu})\nu - N$ scattering is sensitive both to isoscalar and isovector weak currents

and can be a perfect tool to extract G_A^Z without these ambiguities of higher order RCs. The undetermined G_A^Z is typically eliminated from the $(\bar{\nu})\nu - N$ NCE scattering data analysis by imposing a value for Δs determined by differing model assumptions, global analyses, and employing a dipole mass M_A^{dip} obtained from the CCQE $\nu - N$ scattering data analysis. In the latter, G_A^s and the charged current (CC) (through an exchange of W^\pm boson) axial form factor G_A^{CC} are assumed to follow a dipole form. A major goal of this letter is to determine the WNC axial charge $G_A^Z(0)$ and its Q^2 -dependent FF, and hence the s -quark axial charge $G_A^s(Q^2 = 0) \equiv \Delta s$.

Modern neutrino scattering experiments [20–36] are performed with (anti)neutrino scattering off nuclear targets. Along with the challenge of reconstructing incoming neutrino beam energy, these experiments face a defining challenge to systematically consider various nuclear effects in the initial and final-states interactions, and use a combination of various nuclear models to generate the experimental events through Monte-Carlo (MC) simulations (for detailed discussion see Ref. [37]). An accurate determination of $(\bar{\nu})\nu$ interaction with free nucleon is vital to investigate nuclear effects in $(\bar{\nu})\nu$ -nucleus scattering, and effects of various nuclear model inputs in the neutrino scattering experiment MC simulations. In this direction, using our determination of $G_A^Z(Q^2)$, we will reconstruct the MiniBooNE [29, 30] NCE $(\bar{\nu})\nu - N$ scattering differential cross section and provide an accurate prediction of the BNL E734 [20, 21] data in the momentum transfer range of $0 \lesssim Q^2 \leq 1$ GeV².

The $(\bar{\nu})\nu - N$ NCE differential cross-section $d\sigma/dQ^2$, assuming the conservation of vector current [38] which

equates the vector FFs in the EM interaction to the corresponding FFs in the weak interaction, can be written as [39, 40]:

$$\frac{d\sigma_{\nu(\bar{\nu})N \rightarrow \nu(\bar{\nu})N}}{dQ^2} = \frac{G_F^2 Q^2}{2\pi E_\nu^2} (A \pm BW + CW^2), \quad (1)$$

where

$$\begin{aligned} A &= \frac{1}{4}[(G_A^Z)^2(1+\tau) - \{(F_1^Z)^2 - \tau(F_2^Z)^2\}(1-\tau) + 4\tau F_1^Z F_2^Z], \\ B &= -\frac{1}{4}G_A^Z(F_1^Z + F_2^Z), \\ C &= \frac{1}{64\tau}[(G_A^Z)^2 + (F_1^Z)^2 + \tau(F_2^Z)^2], \\ W &= 4(E_\nu/M_p - \tau), \end{aligned} \quad (2)$$

and the $+$ ($-$) sign is for $\nu(\bar{\nu})$ scattering off a free nucleon. Here G_F is the Fermi constant [41], E_ν is the average energy of the neutrino beam, M_p is nucleon mass, and $\tau = Q^2/4M_p^2$.

The WNC Dirac and Pauli FFs $F_{1,2}^Z$ in Eq. (2) can be calculated in terms of the proton and neutron EMFFs $F_{1,2}^{p,n}$ and s -quark FF $F_{1,2}^s$ as

$$\begin{aligned} F_{1,2}^Z &= \left(\frac{1}{2} - \sin^2 \theta_W\right)(F_{1,2}^p - F_{1,2}^n) \\ &\quad - \sin^2 \theta_W(F_{1,2}^p + F_{1,2}^n) - \frac{F_{1,2}^s}{2}. \end{aligned} \quad (3)$$

To calculate $F_{1,2}^Z(Q^2)$, we use the most precise values of $F_{1,2}^s$ obtained from the lattice QCD calculations [42–44] at the physical pion mass and in the continuum and infinite volume limits. While for $F_{1,2}^{p,n}$, we use the most recent model-independent z -expansion fit [45, 46], including two-photon-exchange correction to world electron scattering experimental data from Ref. [47]. With $F_{1,2}^Z(Q^2)$ already determined, we use flux-integrated $d\sigma/dQ^2$ from the MiniBooNE NCE scattering experiments [29, 30] to determine G_A^Z from Eq. (1). Since cross sections are not directly calculable in lattice QCD, for the $d\sigma/dQ^2$ of $(\bar{\nu})\nu - N$ NCE scattering, we have to use experimental data in a limited Q^2 -region as discussed below. It is worth mentioning that, a somewhat similar approach was taken in Ref. [48] to obtain s -quark Sachs EMFFs $G_{E,M}^s$ and Δs .

Since we use $d\sigma/dQ^2$ from MiniBooNE $(\bar{\nu})\nu - N$ scattering experiments in our analysis, we need to keep several limitations in mind. For example, implementation of all possible nuclear effects from different nuclear models in $(\bar{\nu})\nu$ -scattering MC simulations is a daunting task if not impossible at this moment [49–51]. The MC simulator, NUANCE [52] used by the MiniBooNE Collaboration, implemented NCE scattering off free nucleons based on Ref. [53], accounted for the production of intermediate pions [55], the dominance of Pauli-blocking at low Q^2 , and included a model of relativistic

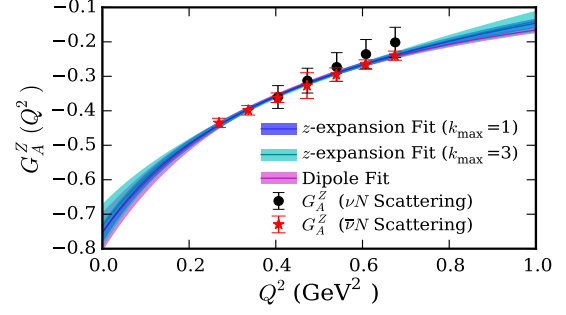


FIG. 1. Neutral current weak axial form factor $G_A^Z(Q^2)$ obtained from analysis combining MiniBooNE data of $(\bar{\nu})\nu - N$ scattering differential cross sections, lattice QCD estimates of s -quark EMFFs, and model-independent z -expansion fit to nucleon EMFFs experimental data. The cyan and blue bands show 2 and 4-terms z -expansion fit to the $G_A^Z(Q^2)$ data, respectively. The magenta band shows a dipole fit to the data.

Fermi gas to account for bound states [54]. Any outgoing pions in NUANCE simulations were given a 20% probability to undergo final-state interaction (FSI).

Instead of a free proton target, MiniBooNE used a mineral-oil (CH_2) based Cherenkov detector, thereby permitting $(\bar{\nu})\nu$ scattering from both bound protons and neutrons in carbon (C), and from free protons in hydrogen (H). To obtain $(\bar{\nu})\nu - N$ -scattering off free nucleons, different efficiency corrections η associated with NCE scattering on free protons (p) in H and on bound protons(neutrons) $p(n)$ in C are combined as:

$$\begin{aligned} \frac{d\sigma_{\nu(\bar{\nu})N \rightarrow \nu(\bar{\nu})N}}{dQ^2} &= \frac{1}{7}\eta_{\nu(\bar{\nu})p,H}(Q^2)\frac{d\sigma_{\nu(\bar{\nu})p \rightarrow \nu(\bar{\nu})p,H}}{dQ^2} \\ &\quad + \frac{3}{7}\eta_{\nu(\bar{\nu})p,C}(Q^2)\frac{d\sigma_{\nu(\bar{\nu})p \rightarrow \nu(\bar{\nu})p,C}}{dQ^2} \\ &\quad + \frac{3}{7}\eta_{\nu(\bar{\nu})n,C}(Q^2)\frac{d\sigma_{\nu(\bar{\nu})n \rightarrow \nu(\bar{\nu})n,C}}{dQ^2} \end{aligned} \quad (4)$$

In our analysis, to avoid possible unknown systematics in η -values, we restrict ourselves to data only in the Q^2 -regions where all three η 's in Eq. (4) are equal to 1 within about 2%, meaning the nuclear effects are small. Furthermore, possible effects of the dipole axial mass M_A^{dip} used as input in the MC simulation are minimized by scattering off a p and n when $\eta \approx 1$. Therefore, for the determination of $G_A^Z(Q^2)$, we consider $d\sigma/dQ^2$ data extracted by MiniBooNE [29, 30] only in the regions $0.40 < Q^2 < 0.68 \text{ GeV}^2$ (for $\nu - N$ scattering) and $0.27 < Q^2 < 0.67 \text{ GeV}^2$ (for $\bar{\nu} - N$ scattering).

The systematic errors are correlated and common to both ν -NCE and $\bar{\nu}$ -NCE scattering measurements by MiniBooNE, and the fit to obtain $G_A^Z(0)$ in the following analysis must be a correlated fit so that the fit uncertainty is not underestimated. Now, with $G_A^Z(Q^2)$

obtained from the combination of experimental and lattice QCD data in the $0.3 \lesssim Q^2 \lesssim 0.7 \text{ GeV}^2$ region as described above, we perform a z -expansion fit [45, 46]:

$$G_A^{Z,z\text{-exp}}(Q^2) = \sum_{k=0}^{k_{\max}} a_k z^k, \quad (5)$$

$$z = \frac{\sqrt{t_{\text{cut}} + Q^2} - \sqrt{t_{\text{cut}}}}{\sqrt{t_{\text{cut}} + Q^2} + \sqrt{t_{\text{cut}}}}$$

to the $G_A^Z(Q^2)$ data to obtain the WNC axial charge $G_A^Z(0)$. We use $t_{\text{cut}} = (3m_\pi)^2$, representing the leading three-pion threshold for states that can be produced by the axial current. We also perform a dipole fit to the data and show the list results of the fit parameters in Table I. As we increase the number of fit param-

z -exp fit	Fit parameters	$G_A^Z(0)$
2-terms	$a_1 = 1.378(92)$	-0.754(26)
3-terms	$a_1 = 1.260(359), a_2 = 0.200(623)$	-0.738(54)
4-terms	$a_1 = 1.248(367), a_2 = 0.127(973), a_3 = 0.201(1.939)$	-0.734(63)
Dipole fit	$M_A^{\text{dip}} = 0.936(53) \text{ GeV}$	-0.752(56)

TABLE I. Parameters of z -expansion fit to Eq.(5) for $G_A^Z(Q^2)$ with 2, 3, and 4 terms. The last row shows results of a dipole fit.

ters, the uncertainties in the higher order coefficients in z -expansion increase and have no signal. However, $a_0 = G_A^Z(0)$ remains the same within the uncertainty. This means that the higher order terms ($k \geq 2$) do not have significant impact on the fit. We consider the z -expansion fit with 4 terms for the subsequent analysis and add the differences in the central values between the 2, 3, and 4-term fits in quadrature as the systematic uncertainty of the fit to obtain a final value

$$G_A^Z = -0.734(63)(20). \quad (6)$$

As shown in Fig. 1, the present calculation does not provide any conclusive evidence for any statistically significant difference between z -expansion and dipole fits. Possible consequences of the $M_A^{\text{dip}} = 0.936(53) \text{ GeV}$ obtained in the dipole fit will be discussed later.

An important result, demonstrated in Fig. 2, is that, although the $G_{E,M}^s$ contribution to the nucleon is much smaller than the valence quark contribution as shown in Refs. [42–44], the assumption of $G_{E,M}^s(Q^2) = 0$ will lead to different results for the nucleon matrix element G_A^Z at the same Q^2 obtained from the anti-neutrino and the neutrino scattering cross section data. Therefore its contribution cannot be ignored as mostly done in previous such calculations.

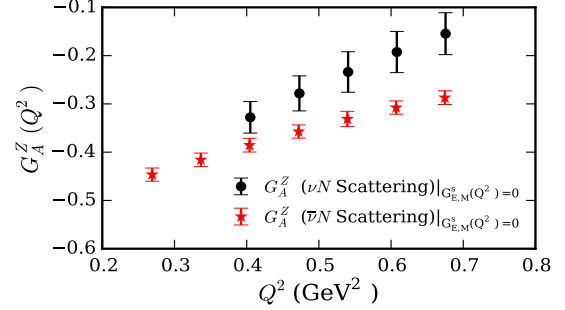


FIG. 2. Neutral current weak axial form factor $G_A^Z(Q^2)$ by assuming zero s -quark contribution $G_{E,M}^s$ leads to inconsistent matrix elements obtained from $\bar{\nu} - N$ and $\nu - N$ scattering.

One can relate G_A^Z with the CC axial FF G_A^{CC} through the s -quark axial FF [39, 40] as

$$G_A^Z = \frac{1}{2}(-G_A^{CC} + G_A^s). \quad (7)$$

With $G_A^{CC}(0) = g_A = 1.2723(23)$ [41] and $G_A^Z(0)$ from Eq. (6), we obtain

$$G_A^s(0) \equiv \Delta s = -0.196(127)(41). \quad (8)$$

The poorly determined uncertainty seen in Δs obtained from Eq. (8) is understood qualitatively through error propagation arguments arising from the cancellation of two large numbers. That said, one important feature of this method is that the $(\bar{\nu})\nu - N$ NCE cross section depends directly on the s -quark contribution, and therefore no assumptions about SU(3) flavor symmetry or fragmentation functions is needed to obtain Δs . We direct the reader for discussion of the influences of SU(3) flavor symmetry in Ref. [58] and fragmentation functions in Ref. [56, 57]). Within the uncertainty, Δs obtained in Eq. (8) is consistent with $\Delta s \sim -0.1$ obtained in global fits [59–64], for example $\Delta s = 0.08(26)$ from MiniBooNE $\nu - N$ NCE scattering [29], and $\Delta s = 0, -0.15(7), -0.13(09), -0.21(10)$, depending on various values of $G_{E,M}^s$, from BNL E734 analysis [40].

With our knowledge of $G_A^Z(Q^2)$ in the $0 \lesssim Q^2 \lesssim 1 \text{ GeV}^2$ kinematic region, Eq. (2) can now be used to obtain the $(\bar{\nu})\nu - N$ differential cross sections as shown in Fig. 3. We are able to successfully reconstruct the MiniBooNE data outside $0.3 \lesssim Q^2 \lesssim 0.7 \text{ GeV}^2$ region that was used for the determination of $G_A^Z(Q^2)$. It is evident from Fig. 3 that in $Q^2 \lesssim 0.15 \text{ GeV}^2$, the free-nucleon scattering prediction starts to deviate from the MiniBooNE result. One reason is that the Pauli blocking effect for which low momentum transfer interactions are suppressed due to occupied phase space. This was already included in the NUANCE MC simulation

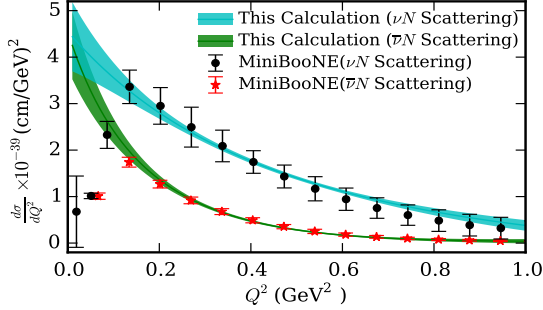


FIG. 3. Comparison of the determination of $(\bar{\nu})\nu - N$ differential cross sections between this calculation and MiniBooNE extractions. The lowest four- Q^2 data points for $\nu - N$ scattering is compiled from Ref. [65].

and showed to have impact exactly in the $Q^2 \lesssim 0.15$ GeV^2 region [66, 67]. Further possible reason is nuclear shadowing which is related to the phenomenon that at low Q^2 , the resolution is not sufficient to resolve a single nucleon wave function and therefore $d\sigma/dQ^2$ decreases [68]. To demonstrate the importance of a correct determination of $G_A^Z(Q^2)$, we show in Fig. 4 that the term $\frac{G_F^2}{2\pi} \frac{Q^2}{E_\nu^2} \frac{1}{64\tau} (G_A^Z)^2 W^2$ has the largest contribution to $d\sigma/dQ^2$ among individual terms in Eq. (1).

Another notable observation is that, in the MiniBooNE NUANCE MC simulation, the values $M_A^{\text{dip}} = 1.23(8)$ for nucleons bound in C, $M_A^{\text{dip}} = 1.13(10)$ GeV for free nucleons, $M_A^{\text{dip}} = 1.10(27)$ GeV for ν -induced resonance pion production, and $M_A^{\text{dip}} = 1.30(52)$ GeV for multi-pion production were used [29, 30]. However, the dipole fit yields $M_A^{\text{dip}} = 0.936(53)$ GeV from the G_A^Z data in our analysis, and the successful reconstruction of the MiniBooNE data in Fig. 3 suggests that the flux-integrated $d\sigma/dQ^2$ for $(\bar{\nu})\nu - N$ scattering is indeed not sensitive to the input of M_A^{dip} in the region where efficiency corrections $C \approx 1$ in Eq. (4). It is worth mentioning that, the higher values of M_A^{dip} in the MC simulation of the experimental data were obtained either to describe a strong suppression of muons in the forward direction [69] or to produce good agreement with the data [28]. NOMAD [24] and MINERvA [33, 34] with $2p-2h$ correction obtained $M_A^{\text{dip}} \sim 1$ GeV , in agreement with the world average [70]. Different model calculations with several of many possible nuclear effects can also describe the MiniBooNE CCQE scattering data still with $M_A^{\text{dip}} \sim 1$ GeV [71–74] (for detailed discussion see Ref. [51]). However, our analysis presented here should not be interpreted as may say anything definitive if or how M_A^{dip} may be modified due to nuclear effects.

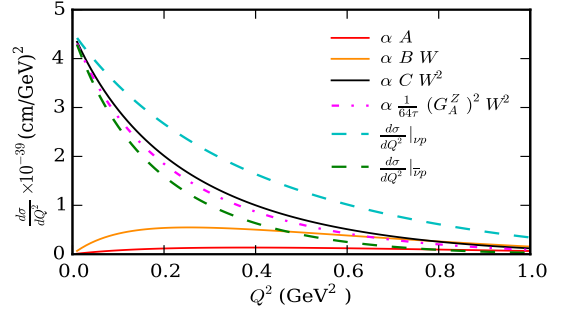


FIG. 4. Contributions from $A(Q^2)$, $B(Q^2)$, $C(Q^2)$ defined in Eq. (2) and $G_A^Z(Q^2)$ to νp and $\bar{\nu} p$ differential cross sections for neutrino beam energy $E_\nu = 1$ GeV . The symbol $\alpha = \frac{G_F^2}{2\pi} \frac{Q^2}{E_\nu^2}$ is used in the figure for shorthand notation.

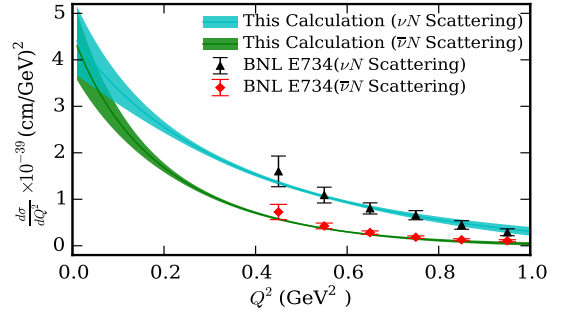


FIG. 5. Prediction of BNL E734 experiment $(\bar{\nu})\nu - N$ differential cross sections.

To test the robustness of our calculation of $G_A^Z(Q^2)$ and $(\bar{\nu})\nu - N$ differential cross sections, and our ability to disentangle nuclear effects, we should be able to describe other independent data.

For this purpose, we now predict the $d\sigma_{\nu(\bar{\nu})N \rightarrow \nu(\bar{\nu})N}/dQ^2$ and compare them with those obtained from BNL E734 experiment for a given $E_\nu = [1.2, 1.3]$ GeV . It is important to mention that none of the BNL E734 data was used in our analysis to obtain G_A^Z , and the experimental data analysis and systematics related to BNL experiment can be different than those of MiniBooNE experiments. As can be seen from Fig. 5, we can successfully predict the BNL E734 $(\bar{\nu})\nu - N$ differential cross sections in the entire available Q^2 -region, demonstrating the validity and predictive power of our determination of $G_A^Z(Q^2)$ and $(\bar{\nu})\nu - N$ differential cross sections using the MiniBooNE data and lattice QCD determinations of $F_{1,2}^s$.

This calculation provides the most precise value of $G_A^Z(Q^2)$. It is demonstrated that $G_A^Z(Q^2)$ is the dominant form factor in $(\bar{\nu})\nu - N$ scattering, and can also be used to isolate the higher order radiative corrections associated with the WNC effective axial form factor in electron-proton parity violating scattering ex-

periments. Although the Δs -value obtained in this analysis has a large uncertainty, it clearly shows a non-zero negative value and is not sensitive to various quark model assumptions and choices of fragmentation functions. Finally, the robustness of this calculation is shown through the predictive power to describe $(\bar{\nu})\nu - N$ differential cross sections from independent experiments. Therefore, this reliable calculation of neutrino-nucleon scattering can have a significant impact in disentangling nuclear effects from the upcoming neutrino-nucleus scattering experiments.

Acknowledgments: RSS thanks Richard Hill who provided the data of the fit to nucleon electromagnetic form factors before the work was published in Ref. [47]. RSS also thanks Colin Egerer and Aaron Meyer. We thank Rajan Gupta, Andreas Kronfeld, , Wally Van Orden, Rocco Schiavilla for useful discussions. This work is supported in part by the U.S. Department of Energy, Office of Science, Office of Nuclear Physics under contract DE-AC05-06OR23177.

-
- [1] K. Abe *et al.* [Super-Kamiokande Collaboration], “Solar neutrino results in Super-Kamiokande-III,” *Phys. Rev. D* **83**, 052010 (2011) [[arXiv:1010.0118 \[hep-ex\]](#)].
 - [2] G. Bellini *et al.*, “Precision measurement of the ^7Be solar neutrino interaction rate in Borexino,” *Phys. Rev. Lett.* **107**, 141302 (2011) [[arXiv:1104.1816 \[hep-ex\]](#)].
 - [3] A. Gando *et al.* [KamLAND Collaboration], “Constraints on θ_{13} from A Three-Flavor Oscillation Analysis of Reactor Antineutrinos at KamLAND,” *Phys. Rev. D* **83**, 052002 (2011) [[arXiv:1009.4771 \[hep-ex\]](#)].
 - [4] P. Adamson *et al.* [MINOS Collaboration], “Measurement of the Neutrino Mass Splitting and Flavor Mixing by MINOS,” *Phys. Rev. Lett.* **106**, 181801 (2011) [[arXiv:1103.0340 \[hep-ex\]](#)].
 - [5] P. Adamson *et al.* [MINOS Collaboration], “First direct observation of muon antineutrino disappearance,” *Phys. Rev. Lett.* **107**, 021801 (2011) [[arXiv:1104.0344 \[hep-ex\]](#)].
 - [6] K. Abe *et al.* [Super-Kamiokande Collaboration], “Search for Differences in Oscillation Parameters for Atmospheric Neutrinos and Antineutrinos at Super-Kamiokande,” *Phys. Rev. Lett.* **107**, 241801 (2011) [[arXiv:1109.1621 \[hep-ex\]](#)].
 - [7] F. P. An *et al.* [Daya Bay Collaboration], “Observation of electron-antineutrino disappearance at Daya Bay,” *Phys. Rev. Lett.* **108**, 171803 (2012) [[arXiv:1203.1669 \[hep-ex\]](#)].
 - [8] J. K. Ahn *et al.* [RENO Collaboration], “Observation of Reactor Electron Antineutrino Disappearance in the RENO Experiment,” *Phys. Rev. Lett.* **108**, 191802 (2012) [[arXiv:1204.0626 \[hep-ex\]](#)].
 - [9] C. A. Bertulani and A. Gade, “Nuclear Astrophysics with Radioactive Beams,” *Phys. Rept.* **485**, 195 (2010) [[arXiv:0909.5693 \[nucl-th\]](#)].
 - [10] C. Volpe, *Annalen Phys.* **525**, no. 8-9, 588 (2013) [[arXiv:1303.1681 \[hep-ph\]](#)].
 - [11] T. Ohlsson, *Rept. Prog. Phys.* **76**, 044201 (2013) [[arXiv:1209.2710 \[hep-ph\]](#)].
 - [12] B. Mueller *et al.* [SAMPLE Collaboration], “Measurement of the proton’s neutral weak magnetic form-factor,” *Phys. Rev. Lett.* **78**, 3824 (1997) [[arXiv:nucl-ex/9702004](#)].
 - [13] D. T. Spayde *et al.* [SAMPLE Collaboration], “The Strange quark contribution to the proton’s magnetic moment,” *Phys. Lett. B* **583**, 79 (2004) [[arXiv:nucl-ex/0312016](#)].
 - [14] D. Androic *et al.* [G0 Collaboration], “Strange Quark Contributions to Parity-Violating Asymmetries in the Backward Angle G0 Electron Scattering Experiment,” *Phys. Rev. Lett.* **104**, 012001 (2010) [[arXiv:0909.5107 \[nucl-ex\]](#)].
 - [15] S. Baunack *et al.*, “Measurement of Strange Quark Contributions to the Vector Form Factors of the Proton at $Q^2 = 0.22 (\text{GeV}/c)^2$,” *Phys. Rev. Lett.* **102**, 151803 (2009) [[arXiv:0903.2733 \[nucl-ex\]](#)].
 - [16] D. Balaguer Rios *et al.*, “Measurement of the parity violating asymmetry in the quasielastic electron-deuteron scattering and improved determination of the magnetic strange form factor and the isovector anapole radiative correction,” *Phys. Rev. D* **94**, no. 5, 051101 (2016).
 - [17] S. L. Zhu, S. J. Puglia, B. R. Holstein and M. J. Ramsey-Musolf, “The Nucleon anapole moment and parity violating e p scattering,” *Phys. Rev. D* **62**, 033008 (2000) [[arXiv:hep-ph/0002252](#)].
 - [18] L. N. Hand, D. G. Miller and R. Wilson, “Electric and Magnetic Form factor of the Nucleon,” *Rev. Mod. Phys.* **35**, 335 (1963).
 - [19] D. Androic *et al.* [Qweak Collaboration], “Precision measurement of the weak charge of the proton,” *Nature* **557**, no. 7704, 207 (2018).
 - [20] J. Horstkotte *et al.*, “Measurement of Neutrino - Proton and Anti-neutrinos - Proton Elastic Scattering,” *Phys. Rev. D* **25**, 2743 (1982).
 - [21] L. A. Ahrens *et al.*, “Measurement of Neutrino - Proton and anti-neutrino - Proton Elastic Scattering,” *Phys. Rev. D* **35**, 785 (1987).
 - [22] S. H. Ahn *et al.* [K2K Collaboration], “Detection of accelerator produced neutrinos at a distance of 250-km,” *Phys. Lett. B* **511**, 178 (2001) [[arXiv:hep-ex/0103001](#)].
 - [23] P. Astier *et al.* [NOMAD Collaboration], “Final NOMAD results on muon-neutrino \rightarrow tau-neutrino and electron-neutrino \rightarrow tau-neutrino oscillations including a new search for tau-neutrino appearance using hadronic tau decays,” *Nucl. Phys. B* **611**, 3 (2001) [[arXiv:hep-ex/0106102](#)].
 - [24] V. Lyubushkin *et al.* [NOMAD Collaboration], “A Study of quasi-elastic muon neutrino and antineutrino scattering in the NOMAD experiment,” *Eur. Phys. J.*

- C **63**, 355 (2009) [[arXiv:0812.4543 \[hep-ex\]](#)].
- [25] P. Adamson *et al.* [MINOS Collaboration], “A Study of Muon Neutrino Disappearance Using the Fermilab Main Injector Neutrino Beam,” *Phys. Rev. D* **77**, 072002 (2008) [[arXiv:0711.0769 \[hep-ex\]](#)].
- [26] P. Adamson *et al.* [MINOS Collaboration], *Phys. Rev. Lett.* **101**, 131802 (2008) [[arXiv:0806.2237 \[hep-ex\]](#)].
- [27] N. Agafonova *et al.* [OPERA Collaboration], “Observation of a first ν_τ candidate in the OPERA experiment in the CNGS beam,” *Phys. Lett. B* **691**, 138 (2010) [[arXiv:1006.1623 \[hep-ex\]](#)].
- [28] A. A. Aguilar-Arevalo *et al.* [MiniBooNE Collaboration], “First Measurement of the Muon Neutrino Charged Current Quasielastic Double Differential Cross Section,” *Phys. Rev. D* **81**, 092005 (2010) [[arXiv:1002.2680 \[hep-ex\]](#)].
- [29] A. A. Aguilar-Arevalo *et al.* [MiniBooNE Collaboration], “Measurement of the Neutrino Neutral-Current Elastic Differential Cross Section on Mineral Oil at $E_\nu \sim 1$ GeV,” *Phys. Rev. D* **82**, 092005 (2010) [[arXiv:1007.4730 \[hep-ex\]](#)].
- [30] A. A. Aguilar-Arevalo *et al.* [MiniBooNE Collaboration], “Measurement of the Antineutrino Neutral-Current Elastic Differential Cross Section,” *Phys. Rev. D* **91**, no. 1, 012004 (2015) [[arXiv:1309.7257 \[hep-ex\]](#)].
- [31] K. Hiraide *et al.* [SciBooNE Collaboration], “Search for Charged Current Coherent Pion Production on Carbon in a Few-GeV Neutrino Beam,” *Phys. Rev. D* **78**, 112004 (2008) [[arXiv:0811.0369 \[hep-ex\]](#)].
- [32] C. Anderson *et al.* [ArgoNeuT Collaboration], “First Measurements of Inclusive Muon Neutrino Charged Current Differential Cross Sections on Argon,” *Phys. Rev. Lett.* **108**, 161802 (2012) [[arXiv:1111.0103 \[hep-ex\]](#)].
- [33] L. Fields *et al.* [MINERvA Collaboration], “Measurement of Muon Antineutrino Quasielastic Scattering on a Hydrocarbon Target at $E_\nu \sim 3.5$ GeV,” *Phys. Rev. Lett.* **111**, no. 2, 022501 (2013) [[arXiv:1305.2234 \[hep-ex\]](#)].
- [34] G. A. Fiorentini *et al.* [MINERvA Collaboration], “Measurement of Muon Neutrino Quasielastic Scattering on a Hydrocarbon Target at $E_\nu \sim 3.5$ GeV,” *Phys. Rev. Lett.* **111**, 022502 (2013) [[arXiv:1305.2243 \[hep-ex\]](#)].
- [35] C. Adams *et al.* [MicroBooNE Collaboration], “Comparison of ν_μ -Ar multiplicity distributions observed by MicroBooNE to GENIE model predictions,” [[arXiv:1805.06887 \[hep-ex\]](#)].
- [36] R. Acciarri *et al.* [DUNE Collaboration], “Long-Baseline Neutrino Facility (LBNF) and Deep Underground Neutrino Experiment (DUNE) : Conceptual Design Report, Volume 2: The Physics Program for DUNE at LBNF,” [[arXiv:1512.06148 \[physics.ins-det\]](#)].
- [37] L. Alvarez-Ruso *et al.*, “NuSTEC 1.1 Neutrino Scattering Theory Experiment Collaboration <http://nustec.fnal.gov> . White Paper: Status and challenges of neutrino?nucleus scattering,” *Prog. Part. Nucl. Phys.* **100**, 1 (2018) [[arXiv:1706.03621 \[hep-ph\]](#)].
- [38] R. P. Feynman and M. Gell-Mann, *Phys. Rev.* **109**, 193 (1958).
- [39] G. Garvey, E. Kolbe, K. Langanke and S. Krewald, “Role of strange quarks in quasielastic neutrino scattering,” *Phys. Rev. C* **48**, 1919 (1993).
- [40] G. T. Garvey, W. C. Louis and D. H. White, “Determination of proton strange form-factors from neutrino p elastic scattering,” *Phys. Rev. C* **48**, 761 (1993).
- [41] C. Patrignani *et al.*, (Particle Data Group), “Review of Particle Physics,” *Chin. Phys.* **C40**, 100001 (2016)
- [42] R. S. Sufian, Y. B. Yang, A. Alexandru, T. Draper, J. Liang and K. F. Liu, “Strange Quark Magnetic Moment of the Nucleon at the Physical Point,” *Phys. Rev. Lett.* **118**, no. 4, 042001 (2017) [[arXiv:1606.07075 \[hep-ph\]](#)].
- [43] R. S. Sufian, “Neutral Weak Form Factors of Proton and Neutron,” *Phys. Rev. D* **96**, no. 9, 093007 (2017) [[arXiv:1611.07031 \[hep-ph\]](#)].
- [44] R. S. Sufian, Y. B. Yang, J. Liang, T. Draper and K. F. Liu, “Sea Quarks Contribution to the Nucleon Magnetic Moment and Charge Radius at the Physical Point,” *Phys. Rev. D* **96**, no. 11, 114504 (2017) [[arXiv:1705.05849 \[hep-lat\]](#)].
- [45] R. J. Hill and G. Paz, “Model independent extraction of the proton charge radius from electron scattering,” *Phys. Rev. D* **82**, 113005 (2010) [[arXiv:1008.4619 \[hep-ph\]](#)].
- [46] Z. Epstein, G. Paz and J. Roy, “Model independent extraction of the proton magnetic radius from electron scattering,” *Phys. Rev. D* **90**, no. 7, 074027 (2014) [[arXiv:1407.5683 \[hep-ph\]](#)].
- [47] Z. Ye, J. Arrington, R. J. Hill and G. Lee, “Proton and neutron electromagnetic form factors and uncertainties,” *Phys. Lett. B* **777**, 8 (2018) [[arXiv:1707.09063 \[nucl-ex\]](#)].
- [48] S. F. Pate, “Determination of the strange form-factors of the nucleon from ν p, $\bar{\nu}$ p, and parity violating polarized-e p elastic scattering,” *Phys. Rev. Lett.* **92**, 082002 (2004) [[arXiv:hep-ex/0310052](#)].
- [49] H. Gallagher, G. Garvey and G. P. Zeller, “Neutrino-nucleus interactions,” *Ann. Rev. Nucl. Part. Sci.* **61**, 355 (2011).
- [50] J. A. Formaggio and G. P. Zeller, “From eV to EeV: Neutrino Cross Sections Across Energy Scales,” *Rev. Mod. Phys.* **84**, 1307 (2012) [[arXiv:1305.7513 \[hep-ex\]](#)].
- [51] L. Alvarez-Ruso, Y. Hayato and J. Nieves, “Progress and open questions in the physics of neutrino cross sections at intermediate energies,” *New J. Phys.* **16**, 075015 (2014) [[arXiv:1403.2673 \[hep-ph\]](#)].
- [52] D. Casper, “The Nuance neutrino physics simulation, and the future,” *Nucl. Phys. Proc. Suppl.* **112**, 161 (2002) [[arXiv:hep-ph/0208030](#)].
- [53] C. H. Llewellyn Smith, “Neutrino Reactions at Accelerator Energies,” *Phys. Rept.* **3**, 261 (1972).
- [54] R. A. Smith and E. J. Moniz, “Neutrino Reactions On Nuclear Targets,” *Nucl. Phys. B* **43**, 605 (1972)

- Erratum: [Nucl. Phys. B **101**, 547 (1975)].
- [55] D. Rein and L. M. Sehgal, “Coherent π^0 Production in Neutrino Reactions,” Nucl. Phys. B **223**, 29 (1983).
 - [56] E. Leader, A. V. Sidorov and D. B. Stamenov, “Determination of Polarized PDFs from a QCD Analysis of Inclusive and Semi-inclusive Deep Inelastic Scattering Data,” Phys. Rev. D **82**, 114018 (2010) [arXiv:1010.0574 [hep-ph]].
 - [57] E. Leader, A. V. Sidorov and D. B. Stamenov, “A Possible Resolution of the Strange Quark Polarization Puzzle ?,” Phys. Rev. D **84**, 014002 (2011) [arXiv:1103.5979 [hep-ph]].
 - [58] J. J. Ethier, N. Sato and W. Melnitchouk, “First simultaneous extraction of spin-dependent parton distributions and fragmentation functions from a global QCD analysis,” Phys. Rev. Lett. **119**, no. 13, 132001 (2017) [arXiv:1705.05889 [hep-ph]].
 - [59] D. de Florian, R. Sassot, M. Stratmann and W. Vogelsang, “Extraction of Spin-Dependent Parton Densities and Their Uncertainties,” Phys. Rev. D **80**, 034030 (2009) [arXiv:0904.3821 [hep-ph]].
 - [60] M. Hirai *et al.* [Asymmetry Analysis Collaboration], “Determination of gluon polarization from deep inelastic scattering and collider data,” Nucl. Phys. B **813**, 106 (2009) [arXiv:0808.0413 [hep-ph]].
 - [61] J. Blumlein and H. Bottcher, “QCD Analysis of Polarized Deep Inelastic Scattering Data,” Nucl. Phys. B **841**, 205 (2010) [arXiv:1005.3113 [hep-ph]].
 - [62] E. R. Nocera *et al.* [NNPDF Collaboration], “A first unbiased global determination of polarized PDFs and their uncertainties,” Nucl. Phys. B **887**, 276 (2014) [arXiv:1406.5539 [hep-ph]].
 - [63] E. Leader, A. V. Sidorov and D. B. Stamenov, “New analysis concerning the strange quark polarization puzzle,” Phys. Rev. D **91**, no. 5, 054017 (2015) [arXiv:1410.1657 [hep-ph]].
 - [64] N. Sato *et al.* [Jefferson Lab Angular Momentum Collaboration], “Iterative Monte Carlo analysis of spin-dependent parton distributions,” Phys. Rev. D **93**, no. 7, 074005 (2016) [arXiv:1601.07782 [hep-ph]].
 - [65] D. Perevalov, “Neutrino-nucleus neutral current elastic interactions measurement in MiniBooNE,” FERMILAB-THESIS-2009-47
 - [66] T. Katori, PhD Thesis [for MiniBooNE Collaboration] “A measurement of the muon neutrino charged current quasielastic interaction and a test of Lorentz violation with the MiniBooNE experiment” FERMILAB-THESIS-2008-64 (2008)
 - [67] A. A. Aguilar-Arevalo *et al.* [MiniBooNE Collaboration], “Measurement of muon neutrino quasi-elastic scattering on carbon,” Phys. Rev. Lett. **100**, 032301 (2008) [arXiv:0706.0926 [hep-ex]].
 - [68] T. Katori and J. Conrad, “Beyond Standard Model Searches in the MiniBooNE Experiment,” Adv. High Energy Phys. **2015**, 362971 (2015) [arXiv:1404.7759 [hep-ex]].
 - [69] R. Gran *et al.* [K2K Collaboration], “Measurement of the quasi-elastic axial vector mass in neutrino-oxygen interactions,” Phys. Rev. D **74**, 052002 (2006) [arXiv:hep-ex/0603034].
 - [70] V. Bernard, L. Elouadrhiri and U. G. Meissner, “Axial structure of the nucleon: Topical Review,” J. Phys. G **28**, R1 (2002) [arXiv:hep-ph/0107088].
 - [71] A. Meucci, M. B. Barbaro, J. A. Caballero, C. Giusti and J. M. Udias, Phys. Rev. Lett. **107**, 172501 (2011) [arXiv:1107.5145 [nucl-th]].
 - [72] M. Martini, M. Ericson, G. Chanfray and J. Marteau, “A Unified approach for nucleon knock-out, coherent and incoherent pion production in neutrino interactions with nuclei,” Phys. Rev. C **80**, 065501 (2009) [arXiv:0910.2622 [nucl-th]].
 - [73] S. Boyd, S. Dytman, E. Hernandez, J. Sobczyk and R. Tacik, “Comparison of models of neutrino-nucleus interactions,” AIP Conf. Proc. **1189**, 60 (2009).
 - [74] J. Nieves, I. Ruiz Simo and M. J. Vicente Vacas, “Inclusive Charged-Current Neutrino-Nucleus Reactions,” Phys. Rev. C **83**, 045501 (2011) [arXiv:1102.2777 [hep-ph]].